

# Characterization of the actin binding properties of the vasodilator-stimulated phosphoprotein VASP

Stefan Hüttelmaier, Birgit Harbeck, Nils Ole Steffens, Tania Meßerschmidt, Susanne Illenberger, Brigitte M. Jockusch\*

*Cell Biology, Zoological Institute, Technical University of Braunschweig, Spielmannstr. 7, D-38092 Braunschweig, Germany*

Received 3 March 1999; received in revised form 12 April 1999

**Abstract** The vasodilator-stimulated phosphoprotein (VASP) colocalizes with the ends of stress fibers in cell-matrix and cell-cell contacts. We report here that bacterially expressed murine VASP directly interacts with skeletal muscle actin in several test systems including cosedimentation, viscometry and polymerization assays. It nucleates actin polymerization and tightly bundles actin filaments. The interaction with actin is salt-sensitive, indicating that the complex formation is primarily based on electrostatic interactions. Actin binding is confined to the C-terminal domain of VASP (EVH2). This domain, when expressed as a fusion protein with EGFP, associates with stress fibers in transiently transfected cells.

© 1999 Federation of European Biochemical Societies.

**Key words:** Vasodilator-stimulated phosphoprotein; Actin binding protein; Focal contact; Microfilament organization

## 1. Introduction

The vasodilator-stimulated phosphoprotein VASP was originally described as a major substrate for cAMP- and cGMP-dependent protein kinases in human platelets [1], and is thought to participate in the regulation of platelet aggregation [2]. This view is supported by recent data showing that in VASP knock-out mice collagen-induced platelet aggregation is significantly altered [3]. Structural data on VASP are still lacking, but the human protein, comprising 380 amino acids, is organized in three functional domains: an N-terminal EVH1 (residues 1–113), a proline-rich central (residues 114–225) and a C-terminal EVH2 (residues 226–380) domain. A schematic view of this domain organization is shown in Hüttelmaier et al. [4]. In a variety of cells, VASP was found localized at the cytoplasmic face of cell-cell and cell-matrix contact sites, and in vitro data revealed that it is a multiligand protein interacting with a variety of microfilament proteins which colocalize with VASP in these areas, like zyxin [5], vinculin [6,7] and profilin [8]. For vinculin, complex formation with VASP has been demonstrated in living cells and both proteins have been shown to concentrate in nascent cell-matrix junctions during cell spreading [4]. Actin binding of partially phosphorylated VASP, obtained from human platelets and as a recombinant protein from insect cells, has been reported [9,10], but the nature of this interaction has not been investigated in detail.

In this study, we show that bacterially expressed and purified murine VASP, equipped with a his tag, interacts with muscle actin in a variety of in vitro assays. It acts as a nucleator of actin polymerization, cosediments with prepolymerized actin filaments and bundles them tightly. Actin binding was seen to strongly depend on the ionic strength of the solution, indicating that complex formation between VASP and actin is based on electrostatic interactions, and was found to reside in the EVH2 domain. In fibroblasts transiently transfected with EGFP (enhanced green fluorescent protein) fusion proteins, with the EGFP part located at the N-terminus of either VASP or its domains, the full length protein targeted to cell-matrix contact sites, while the EVH2 domain decorated stress fibers.

## 2. Materials and methods

### 2.1. Cloning of murine VASP and its derivatives

Murine VASP and its EVH1 and EVH2 domains were generated by PCR using a VASP EST clone (GenBank accession number W45954, IMAGEp 998J10814, RZPD, Berlin). Amplification primers contained a 5' *EcoRI* and a 3' *XhoI* restriction site for further subcloning into vectors for expression of recombinant his-tagged proteins in bacteria (pQE-30, Qiagen, Hilden, Germany) or transfection experiments with fluorescent proteins in fibroblasts (pEGFP-C2, Clontech, Palo Alto, CA, USA). Amplification primers were designed so that full length VASP contained amino acids 1–375, EVH1 amino acids 1–113 and EVH2 amino acids 222–375. In contrast to human VASP, murine VASP comprises only 375 amino acids based on a four amino acid deletion in the proline-rich region and a single amino acid deletion in the EVH2 domain. In addition, sequencing of the murine EST clone revealed two deviations from the corresponding GenBank entry: amino acid 209 contained alanine (GCA) instead of threonine (ACA) and amino acid 288 (glutamine) was deleted.

For detection purposes, the vectors encoding his-tagged proteins were equipped with further tags. To the N-terminus of full length VASP, an 11 amino acid motif of birch profilin was added (BiPro-tag) which is specifically recognized by a monoclonal antibody against this plant protein [11]. EVH1 and EVH2 domains were equipped with a Flag-tag sequence (Sigma, Munich, Germany).

### 2.2. Protein expression, purification and analysis

For recombinant expression of his-tagged proteins, *Escherichia coli* (M 15) were transformed with the vectors pQE-30-BiPro-VASP, pQE-30-Flag-EVH1 and pQE-30-Flag-EVH2 and grown in 2 × YT medium at 30°C. Protein expression was induced and proteins were purified essentially as described in the manufacturer's protocol (Qiagen, Hilden, Germany). Additional purification was achieved by FPLC (Pharmacia, Uppsala, Sweden) on a Mono S column in 0.05 M sodium phosphate, pH 6.7, 0.1 M KCl, 20 mM β-mercaptoethanol, 0.46 μM aprotinin and 100 μM pefabloc SC, using a KCl gradient for protein elution. Skeletal muscle actin was prepared from acetone powder as described and used as Mg<sup>2+</sup>-actin [12]. Purity of all protein preparations was routinely checked by SDS-PAGE and immunoblots using antibodies against BiPro- and Flag-tag. Protein concentration was determined by the Bradford method [13].

\*Corresponding author. Fax: (49) (531) 391 8203.  
E-mail: bmj@tu-bs.de

### 2.3. Actin binding assays

For sedimentation assays, 20  $\mu$ M actin was prepolymerized in buffer A (0.025 M Na-phosphate, pH 7.0, 1 mM ATP, 0.5 mM EGTA, 0.5 mM dithioerythritol, 2 mM MgCl<sub>2</sub>, and KCl concentrations varying between 15 and 150 mM) for 2 h at 37°C and incubated with VASP or its domains for 1 h at room temperature. Sedimentation assays were performed in an airfuge as described [14], with 2  $\mu$ M actin as a final concentration. Supernatants and sediments were analyzed by SDS-PAGE.

Complex formation of VASP with actin was monitored with pyrene-labeled actin (10% of the total actin) essentially as described [15]. After equilibrating purified actin in buffer B (0.025 M HEPES, pH 7.0, 0.2 mM CaCl<sub>2</sub>, 0.5 mM DTE, 1 mM ATP) for 30 min at 25°C, VASP or its domains were added and polymerization was started by adjusting the solution to 0.025 M NaCl, 2 mM MgCl<sub>2</sub>, and KCl concentrations between 15 and 150 mM. The kinetics of the reaction were followed for 1 h. After an additional 12 h, aliquots from the same samples were used for sedimentation at 100 000  $\times g$  (high speed) in an airfuge or at 12 000  $\times g$  in an eppifuge (low speed), to monitor the presence of F-actin [14] and F-actin bundles [16], respectively.

Actin filament crosslinking and bundling by VASP and its domains was probed by low shear viscometry essentially as described [12,17], with some modifications. Proteins were added to a 3  $\mu$ M prepolymerized F-actin solution in buffer C (0.025 M HEPES, pH 7.0, 0.2 mM CaCl<sub>2</sub>, 0.5 mM DTE, 1 mM ATP, 0.025 mM NaCl, 2 mM MgCl<sub>2</sub>, KCl (15 mM, 50 mM or 150 mM), 0.46  $\mu$ M aprotinin and 100  $\mu$ M pefabloc SC). Aliquots were transferred to glass capillaries and left to equilibrate at room temperature overnight. Relative viscosity of the samples was determined as the time needed for a steel ball to pass a standard distance in the capillary, and expressed in relation to a control containing only F-actin. VASP- and EVH2-induced, rhodamine-phalloidin-labeled actin bundles were obtained and examined essentially as described in [17], except that all components were mixed before polymerization was induced, and fixation was omitted.

### 2.4. Localization of exogenous VASP and its domains in transfected cells

NIH 3T3 fibroblasts were grown in Dulbecco's MEM supplemented with 10% fetal calf serum at 10% CO<sub>2</sub>. For analysis of expression and localization of exogenous proteins, cells were seeded overnight onto collagen-coated coverslips and transfected with calcium phosphate precipitates of the eukaryotic vectors coding for EGFP-VASP constructs (pEGFP-C2, Clontech, with corresponding inserts), according to standard protocols. Forty-eight hours after transfection, cells were washed three times with phosphate-buffered saline containing 2 mM MgCl<sub>2</sub> and 10% glycerol and fixed with the bifunctional membrane-permeable crosslinker DSP (Pierce, Rockford, IL, USA) for 30 min at 37°C [18,19]. After additional washing, cells were permeabilized with 0.2% Triton X-100 and excess crosslinker was quenched with 0.2 M glycine. Counterstaining for F-actin and fluorescence microscopy were performed as described [4].

## 3. Results

### 3.1. Recombinant murine VASP and its isolated C-terminal domain (EVH2) display salt-dependent actin binding

When mixed with G-actin and pyrenyl-labeled G-actin in buffers promoting actin polymerization, the bacterially expressed VASP was shown to increase the fluorescence intensity of the sample (Fig. 1A), in a concentration-dependent manner (not shown). As the increase in pyrenyl-actin fluorescence indicates protein complex formation, the results of these experiments might reflect either that VASP forms complexes with G-actin, or that VASP acts as a nucleator, stabilizing actin seeds and therefore increasing the velocity of actin polymerization. As seen in Fig. 1B, the latter interpretation is

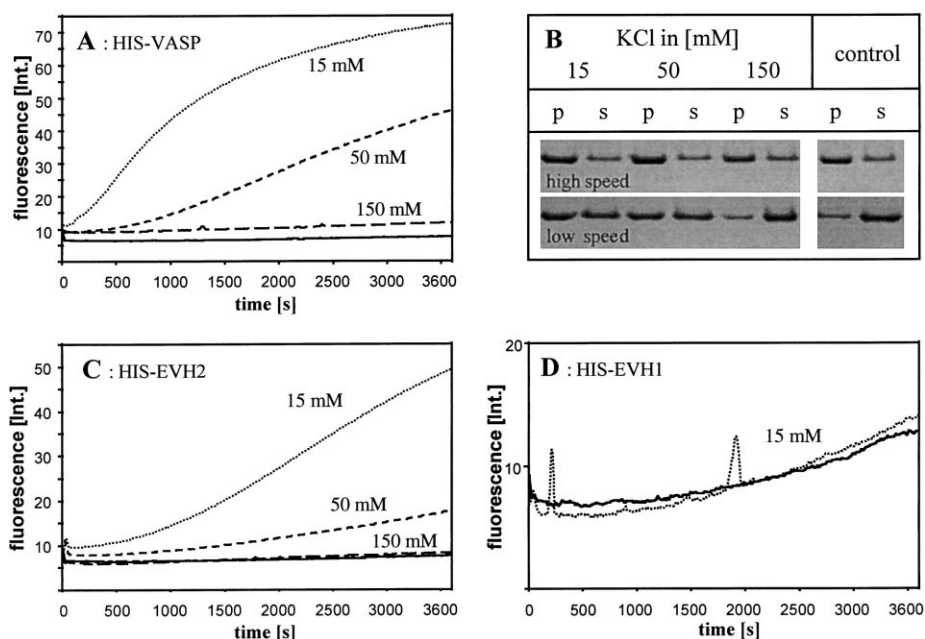


Fig. 1. Effect of VASP and its domains on the polymerization of actin. A, C, D: Fluorescence spectroscopy, following the polymerization of pyrenyl-labeled actin in the absence and presence of VASP (A) and the EVH1 (D) and EVH2 (C) domains. Final concentrations of the solutions were 1  $\mu$ M G-actin, 0.25  $\mu$ M VASP (A), 1  $\mu$ M EVH2 (C) or 1  $\mu$ M EVH1 (D), containing different KCl concentrations as indicated. The actin controls (solid lines) were incubated in 15 (D) or 150 (A, C) mM KCl only. The effect of VASP on actin fluorescence is stronger than that of EVH2, while EVH1 is ineffective. Note the difference in ordinate scale between A/C and D. B: SDS-PAGE analysis of aliquots taken from A after 12 h additional incubation. Coomassie-stained actin bands are shown in the pellets (p) and supernatants (s) obtained after high speed and low speed centrifugation. Note that the fraction of pelletable actin in the presence of VASP (left part of B, low speed centrifugation) correlates inversely with the salt concentration and that at 15 mM KCl, it is higher than in the actin control. This indicates that the effect of VASP on actin fluorescence is due to a salt-sensitive nucleating and bundling activity.

correct: VASP was found to increase rather than decrease the amount of sedimentable actin in these samples, as compared with the actin control. A substantial proportion of the filaments formed was also sedimented after low speed centrifugation, indicating that bundling of the filaments had occurred (Fig. 1B). As seen in Fig. 1A,B, the interaction of VASP with actin was found to strongly depend on the ionic strength of the buffer. At low salt conditions (15 mM KCl, 25 mM NaCl and 2 mM MgCl<sub>2</sub>), the effect on actin polymerization kinetics was much stronger than at higher KCl concentrations (i.e. using 50 mM KCl as a medium, 150 mM KCl as a high salt concentration). At low KCl concentrations, a molar ratio of VASP to actin of 0.25:1 led to a prominent stimulation of polymerization, approaching saturation levels within 1 h (Fig. 1A). When the N- and C-terminal domains of VASP, EVH1 and EVH2, were probed separately with respect to their interaction with actin, only the EVH2 domain was found to be reactive (Fig. 1C). Its influence on pyrenyl-actin fluorescence was significantly lower than that of the full length protein. At 1 μM concentrations of both EVH2 and actin (i.e. equimolar amounts), the effect on fluorescence was still less prominent than that measured for VASP at one fourth of this concentration (compare Fig. 1A with C), but again the interaction

with actin was strongly salt-dependent. The EVH1 domain did not display actin binding activity in this assay (Fig. 1D). The polymerization velocity of the actin control itself was also salt-dependent, being slightly slower at high KCl values than at lower ones (not shown), but this effect was negligible in comparison with the effect of VASP and EVH2 on actin polymerization.

### 3.2. Recombinant VASP and the EVH2 domain bind to actin filaments in a salt-dependent manner

Binding of recombinant murine VASP and its domains to prepolymerized F-actin was analyzed using rabbit skeletal muscle actin in sedimentation assays. Fig. 2 shows the protein composition of supernatants and pellets obtained after high speed centrifugation of equimolar mixtures of F-actin and VASP, EVH1 or EVH2, in the presence of increasing KCl concentrations (15 mM, 50 mM or 150 mM). Recombinant VASP (Fig. 2A) and EVH2 (Fig. 2B) cosedimented with preformed F-actin under low salt conditions, demonstrating that VASP and its EVH2 domain not only interact with F-actin during polymerization (cf. Fig. 1A,C), but also interact with preexisting filaments. Under the same buffer conditions, less EVH2 sedimented with actin as compared to VASP (cf. Fig. 2A with B), suggesting that EVH2 binding to F-actin may be less efficient than that of full length VASP. Increasing the KCl concentrations reduced the amount of both proteins cosedimenting with actin (Fig. 2A,B). As already seen in the fluorescence assay with pyrenyl-actin, the EVH1 domain showed no actin binding activity (Fig. 2C).

### 3.3. Recombinant VASP and EVH2 bundle actin filaments

The nature of the binding of VASP to F-actin was further analyzed by low shear viscometry, using a falling ball viscometer. Prepolymerized actin, used as a control, displays a high viscosity (relative viscosity 1.0, Fig. 3A), due to F-actin network formation. At low KCl concentrations, and in the presence of increasing amounts of either VASP or EVH2, this viscosity value decreases dramatically, with EVH2 being somewhat less effective than intact VASP (Fig. 3A). At a molar ratio of 0.2:1 (VASP/EVH2:actin), the relative viscosity was only approximately one tenth of that of the actin control, and at the ratio of 0.5:1, the relative viscosity approached extremely low levels. In contrast, the EVH1 domain showed only a slight effect on the actin viscosity (Fig. 3A), confirming also in this assay the results obtained by fluorescence spectroscopy and sedimentation.

Salt dependence of the actin bundling activity of VASP and EVH2 was determined as shown in Fig. 3B. Under low salt conditions, at molar ratios where the low shear viscosity of a mixture of VASP or EVH2 with actin was very low (0.3:1), increasing KCl concentrations were found to positively correlate with an increase in viscosity. At high ionic strength, the relative viscosity of the samples was only slightly lower than that of the actin control, indicating that under these conditions, little VASP/EVH2 was bound to F-actin. As expected from the results described above, the EVH1 domain had no substantial effect on actin viscosity at different salt conditions (not shown).

Since the sedimentation assays clearly showed that neither VASP nor EVH2 interferes with the integrity of actin filaments, the VASP/EVH2-induced decrease in F-actin viscosity does not reflect fragmentation or depolymerization of actin.

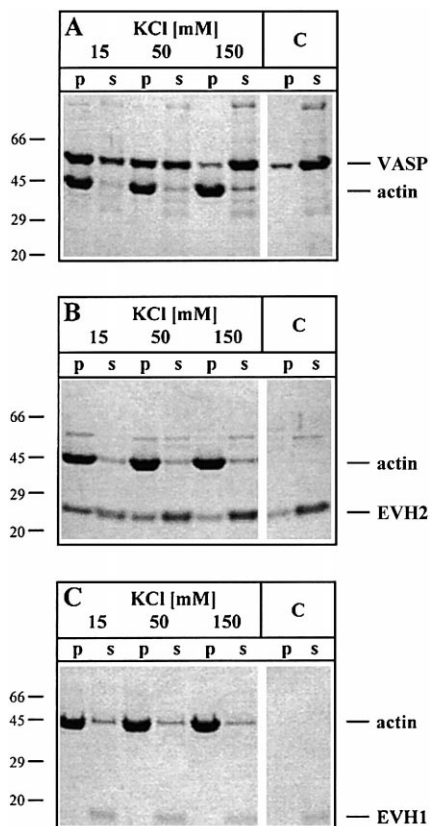


Fig. 2. Sedimentation assays of prepolymerized F-actin (2 μM) with 2 μM VASP (A), 2 μM EVH2 (B) and 2 μM EVH1 (C). The samples were adjusted to the different KCl concentrations as indicated, centrifuged, and pellets and supernatants were processed for SDS-PAGE. VASP as well as EVH2 cosediment with F-actin, while EVH1 does not. Complex formation is most efficient at low KCl concentration, and VASP binds more efficiently than EVH2. C: Control samples without actin, to demonstrate that sedimentation of the recombinant proteins alone is negligible.

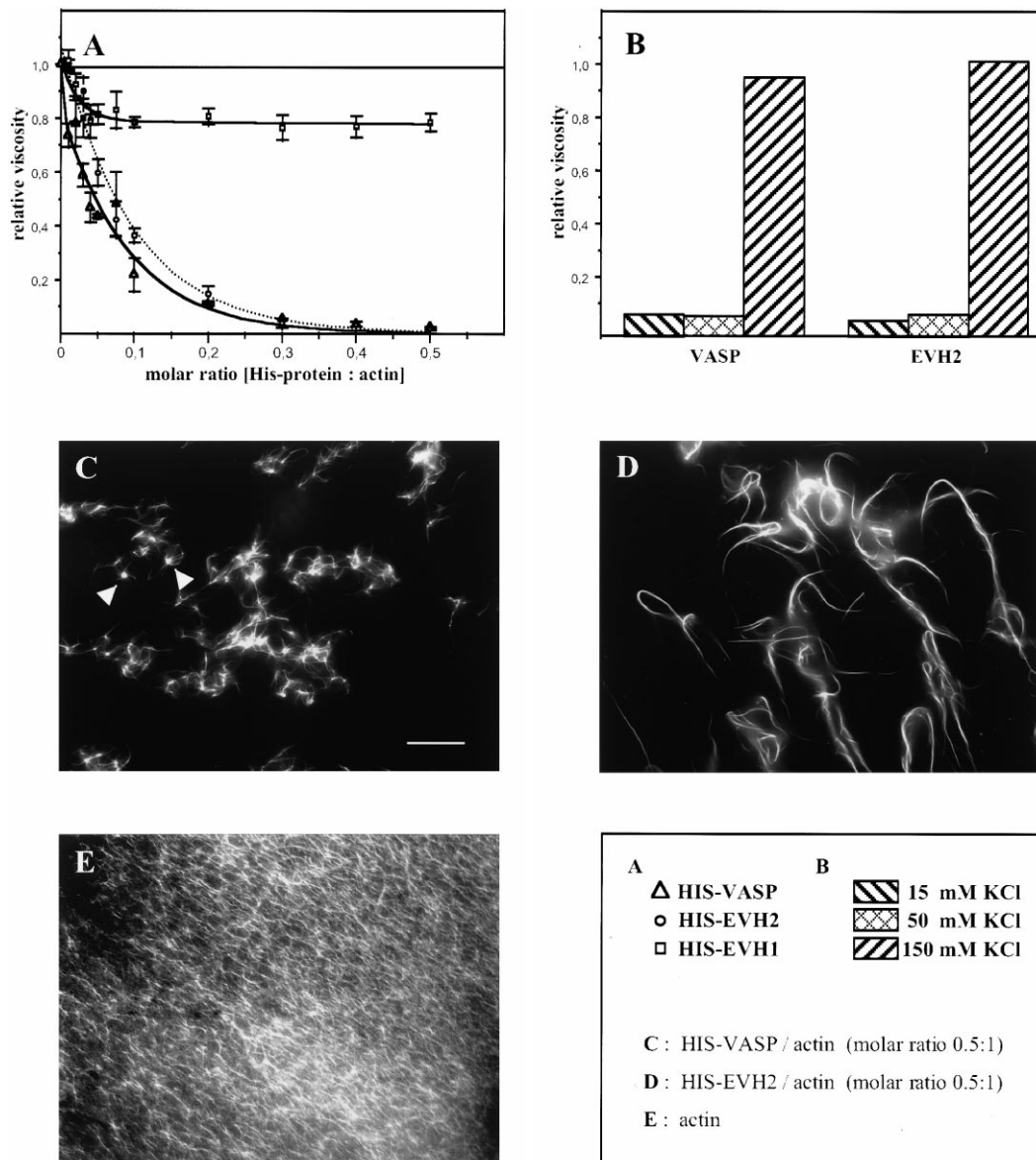


Fig. 3. Formation of actin bundles by VASP and EVH2. A, B: Low shear viscometry of prepolymerized actin (3  $\mu$ M) in the presence and absence of VASP, EVH1 and EVH2, as indicated. The relative viscosity of the actin control (solid line in A) is set at 1.0. A: Viscosity as a function of VASP and EVH1/EVH2 concentration. Note the dramatic decrease of viscosity already at very low concentrations of VASP or EVH2, in contrast to the high viscosity in the presence of EVH1. B: Viscosity as a function of the salt conditions, measured with mixtures of prepolymerized actin (3  $\mu$ M) and 1  $\mu$ M VASP or EVH2. Note the prominent salt dependence of the low shear viscosity. C–E: Fluorescence microscopy of TRITC-phalloidin-labeled actin filaments, polymerized in the presence of the indicated proteins. Note the strong bundling activity of both VASP and EVH2, explaining the drastic decrease in viscosity (A), in contrast to the web-like texture of the F-actin control (E). For the difference in morphology between the bundles in C and D, see text. Bar: 10  $\mu$ m.

Instead, it indicates the formation of tight actin bundles which retain the falling ball much less than the F-actin control. This has been shown previously for  $Mg^{2+}$  actin paracrystals, and for actin bundles induced by vinculin and  $\alpha$ -actinin [12,17,20]. When we examined rhodamine-phalloidin-labeled actin filaments, formed in the presence of either VASP or EVH2, by fluorescence microscopy, the bundles were easily visualized (Fig. 3C,D), while the actin control showed a fine network instead (Fig. 3E). Hence, VASP and the EVH2 domain both display a potent actin bundling activity. However, the morphology of the bundles differed between VASP and the EVH2 domain: VASP induced numerous star-like aggregates, with short bundles radiating from a distinct center (Fig. 3C, arrow-

heads), while EVH2 led to the formation of long, flexible bundles (Fig. 3D).

#### 3.4. In transfected cells, exogenous VASP and EVH2 are both associated with the microfilament system but target to different locations

The results of the in vitro experiments described above suggested a salt-dependent and therefore primarily electrostatic interaction between VASP and actin filaments, residing mainly or exclusively in the EVH2 domain. To characterize such interactions under more physiological conditions, we transiently transfected 3T3 fibroblasts with VASP, EVH1 and EVH2 bearing a GFP variant (EGFP) at their N-termini,

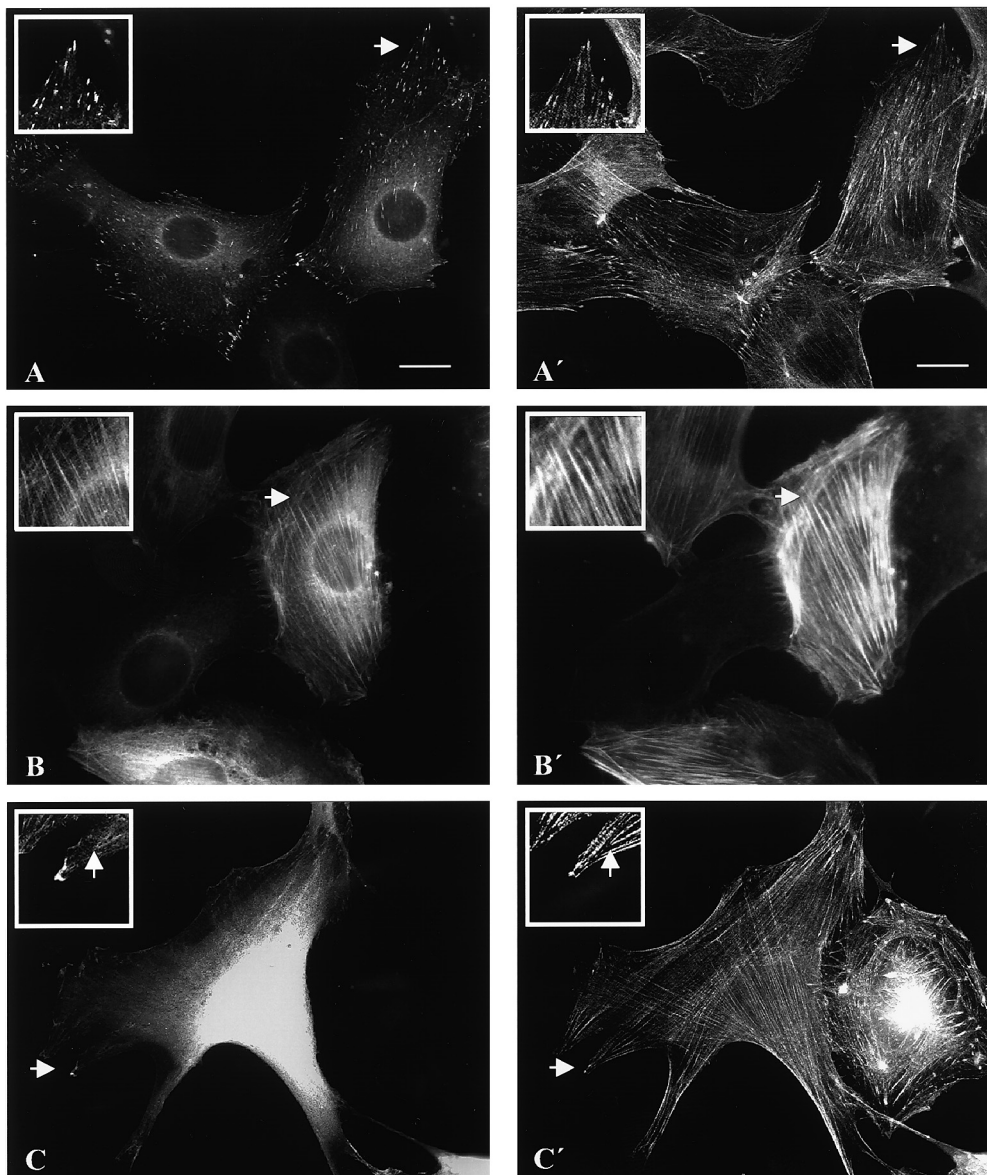


Fig. 4. Fluorescence microscopy of 3T3 fibroblasts transiently transfected with EGFP-fusion proteins of VASP, EVH1 and EVH2. Double fluorescence images for EGFP-VASP (A), EGFP-EVH2 (B) and EGFP-EVH1 (C) are shown, where F-actin is counterstained with rhodamine phalloidin (A', B', C'). The arrowheads point to the regions enlarged in the insets. Note the targeting of VASP to focal contact sites (A,A'), the homogeneous decoration by EVH2 (B,B') of stress fibers which appear thicker than normal (cf. the transfected cells in B' with A' and C'), and the rather homogeneous distribution of EVH1 (C,C'), with an occasional weak decoration of stress fiber ends at a focal contact (small arrowhead, inset in C,C'). Bar: 10  $\mu$ m.

which allows direct detection of the exogenous proteins in the host cells. We then analyzed the localization of the exogenous protein in fixed cells by fluorescence microscopy. Fig. 4 shows the results of such experiments. Full length VASP (Fig. 4A) targeted primarily to the ends of stress fibers at focal contact sites, in accordance with the high concentration of the endogenous protein seen at the same sites in non-transfected cells (cf. [4,9]). In contrast, the transfected EVH2 domain decorated stress fibers along their entire length (Fig. 4B), but was not seen in cell adhesion sites, as confirmed by counterstaining for zyxin (data not shown). In general, stress fibers in cells expressing high levels of the EVH2 domain appeared thicker than in control or VASP-transfected cells. The exogenous EVH1 domain was seen rather homogeneously distributed throughout the cytoplasm and the nucleus (Fig. 4C).

Only occasionally, in well spread cells expressing moderate levels of the protein, a weak staining of stress fiber ends at some focal contacts was seen (Fig. 4C, inset).

#### 4. Discussion

In this study we present a detailed analysis of the interaction of bacterially expressed murine VASP with actin. For the *in vitro* assays, we used his-tagged VASP rather than a GST-fusion protein, to avoid a possible influence of the GST part on protein interactions. Furthermore, by using the recombinant protein, we could exclude the influence of posttranslational modification of VASP on the interaction with actin. In previous reports [9,10], a mixture of unphosphorylated and phosphorylated VASP was used to show F-actin binding.

A prominent nucleating activity of VASP during actin polymerization was revealed by fluorescence spectroscopy in combination with sedimentation assays, but this method does not answer the question whether VASP binds solely to actin in the F-conformation (as for example present in actin nuclei and filaments), or, additionally, to G-actin. Both may be possible, but VASP is certainly primarily an F-actin nucleating protein, not a G-actin sequestering protein.

VASP binds to preformed actin filaments and organizes them into tight bundles. This was already concluded from sedimentation [9,10] and turbidity measurements [10], but a detailed analysis of the bundling activity as a function of the VASP:actin ratio and the ionic strength of the buffer has not been presented. Our data show that both VASP and its isolated actin binding domain EVH2 induce F-actin bundles, when present during actin polymerization. VASP, being the more effective nucleator, organizes actin filaments into star-like aggregates, while EVH2 aligns the filaments into parallel bundles.

For actin bundling proteins in general, two alternative mechanisms can be envisioned. According to the conventional mode, bundling proteins also display a filament crosslinking activity, either due to more than one actin binding motif per polypeptide, or due to dimer or oligomer formation between polypeptides comprising one actin binding motif each. Vinculin, which has two actin binding motifs, and  $\alpha$ -actinin, which is a homodimer with one actin binding site per polypeptide chain, are examples of this case, and both these proteins show a crosslinking activity at low molar ratios to actin (0.2:1 for  $\alpha$ -actinin, and 0.5:1 for vinculin) but a bundling activity seen at ratios above these values [12,17,20]. Vinculin-actin complexes are stably formed within a wide range of buffers of different ionic strengths, indicating that this interaction does not primarily depend on ionic interactions [14].

The alternative mode for bundling does not require more than one actin binding motif but creates filament bundles by electrostatic interactions between a basic motif of the bundling protein and the acidic actin subunits in the filament. In this case, the interactions neutralize surface charges at the filaments, which is apparently sufficient for bundling and does not require crosslinking. In this context, it is noteworthy that VASP and EVH2 both are very effective in actin bundling and show no crosslinking activity, as revealed by the steep decrease of low shear viscosity already at very low ratios to actin (0.01:1, see Fig. 3A). An example of a protein bundling filaments solely by electrostatic interaction is the smooth muscle protein calponin which, quite similar to VASP, nucleates actin polymerization and bundles filaments in a strictly salt-dependent manner [16]. In low salt buffers, i.e. under conditions in which it interacts with actin, calponin is monomeric [21]. For VASP, information on its molecular state in solution or when bound to actin is still lacking. It has been reported that purified VASP exists as a tetramer [22], but in our hands monomeric, dimeric, tetrameric and higher aggregates were found after chemical crosslinking of VASP in solution as well as in cells (data not shown). Due to these observations, one might wonder whether the electrostatic interaction might indeed be confined to the interaction with actin, or involve also a VASP oligomerization process. As the ratio of oligomeric products obtained after chemical crosslinking of purified VASP was not affected by increasing the KCl concentration from 15 to 150 mM (data not shown), we sug-

gest that it is indeed primarily the complex formation with actin which is sensitive to high ionic strength. VASP displays an isoelectric point (IEP) of 8.53, and the EVH2 domain an IEP of 8.1, which would be sufficient for a strong electrostatic interaction with actin, but the EVH1 domain, which proved inactive in our assays, is even more basic, showing an IEP of 9.4 (our own unpublished data).

However, these considerations do not preclude the possibility that small basic clusters, surface exposed within a larger domain of any IEP, might mediate electrostatic actin binding. While our data demonstrate that the EVH2 domain alone, in contrast to EVH1, has actin binding and bundling activity, we cannot exclude further actin binding motifs in the VASP sequence, for example within the central proline-rich domain. This portion of the VASP molecule is unstable and cannot be isolated from bacteria as a discrete entity. The weaker nucleating effect of the EVH2 domain on actin, as compared to the full length VASP, and the observed difference in VASP-actin and EVH2-actin bundle morphology, may reflect some regulatory influence of the intact protein on the activity of this domain.

In an attempt to compare the *in vitro* binding capacity of VASP with a more physiological situation, we examined the possible association of VASP and the EVH domains with actin filaments in transfected cells. 3T3 fibroblasts expressed the respective GFP-tagged constructs and could thus be used to analyze the targeting of the exogenous proteins. Full length VASP was seen concentrated in focal contacts, in accordance with the location of the endogenous protein, but was not seen along stress fibers. This may reflect the fact that the N-terminal EHV1 domain of VASP, when present in the intact protein, interacts with two focal contact proteins, vinculin [6] and zyxin [5], and that these interactions may be of higher affinity than that with actin. Alternatively or additionally, ligand binding activities of VASP may be subject to regulatory mechanisms, for example by phosphorylation.

The exogenous EVH2 domain was clearly seen to decorate stress fibers. Even in cells expressing this fragment to very high levels, we did not observe a gross reorganization of filamentous actin into abnormal tangles or needles, as for example observed in cells transfected with the vinculin actin binding fragment [12]. We cannot exclude that the stress fiber decoration by the EHV2 domain involves binding to stress fiber constituents other than F-actin. However, the observation that, in general, stress fibers in EVH2-transfected cells appeared thicker than normal suggests a direct interaction between EVH2 and F-actin, resulting in actin filament bundling comparable to that seen *in vitro*. Thickening of stress fibers might then indicate the recruitment of filamentous actin to the preexisting fibers by electrostatic interactions, in a zipper-like mechanism. Further analysis of this phenomenon with mutant domains is in progress.

Considering the prominent salt sensitivity of the interaction of VASP and EVH2 with actin, as observed *in vitro*, the observed association of both these proteins with actin filaments at the physiological ionic strength in cells remains to be explained. In this context, it should be mentioned that calponin, which *in vitro* bundles F-actin also exclusively at low ionic strength [16], was found associated with the actin cytoskeleton in activated platelets and with stress fibers in fibroblasts [23], and with the contractile and cytoskeletal compartment of smooth muscle cells [23,24]. For this protein, it

has been proposed that the local concentration of actin and calponin within such structures may be sufficiently high to allow for complex formation even under the conditions of the cytoplasm [16]. An analogous explanation may be assumed for VASP.

*Acknowledgements:* This work was supported by the Deutsche Forschungsgemeinschaft.

## References

- [1] Halbrugge, M. and Walter, U. (1990) *J. Chromatogr.* 521, 335–343.
- [2] Walter, U., Eigenthaler, M., Geiger, J. and Reinhard, M. (1993) *Adv. Exp. Med. Biol.* 344, 237–249.
- [3] Aszödi, A. et al. (1999) *EMBO J.* 18, 37–48.
- [4] Hüttelmaier, S., Mayboroda, O., Harbeck, B., Jarchau, T., Jockusch, B.M. and Rüdiger, M. (1998) *Curr. Biol.* 8, 479–488.
- [5] Reinhard, M., Jouvenal, K., Tripier, D. and Walter, U. (1995) *Proc. Natl. Acad. Sci. USA* 92, 7956–7960.
- [6] Reinhard, M., Rüdiger, M., Jockusch, B.M. and Walter, U. (1996) *FEBS Lett.* 399, 103–107.
- [7] Brindle, N.P.J., Holt, M.R., Davies, J.E., Price, C.J. and Critchley, D.R. (1996) *Biochem. J.* 318, 753–757.
- [8] Reinhard, M., Giehl, K., Abel, K., Haffner, C., Jarchau, T., Hoppe, V., Jockusch, B.M. and Walter, U. (1995) *EMBO J.* 14, 1583–1589.
- [9] Reinhard, M., Halbrugge, M., Scheer, U., Wiegand, C., Jockusch, B.M. and Walter, U. (1992) *EMBO J.* 11, 2063–2070.
- [10] Laurent, V., Loisel, T.P., Harbeck, B., Wehman, A., Gröbe, L., Jockusch, B.M., Wehland, J., Gertler, F. and Carlier, M.F. (1999) *J. Cell Biol.* (in press).
- [11] Rüdiger, M., Jockusch, B.M. and Rothkegel, M. (1997) *BioTechniques* 23, 96–97.
- [12] Rüdiger, M., Korneeva, N., Schwienbacher, C., Weiss, E.E. and Jockusch, B.M. (1998) *FEBS Lett.* 431, 49–54.
- [13] Bradford, M.M. (1976) *Anal. Biochem.* 72, 248–254.
- [14] Menkel, A.R., Kroemker, M., Bubeck, P., Ronsiek, M., Nikolai, G. and Jockusch, B.M. (1994) *J. Cell Biol.* 126, 1231–1240.
- [15] Schlüter, K., Schleicher, M. and Jockusch, B.M. (1998) *J. Cell Sci.* 111, 3261–3273.
- [16] Tang, J.X., Szymanski, P., Janmey, P.A. and Tao, T. (1997) *Eur. J. Biochem.* 247, 432–440.
- [17] Korneeva, N.L. and Jockusch, B.M. (1996) *Eur. J. Cell Biol.* 71, 351–355.
- [18] Hinck, L., Nathke, I.S., Papkoff, J. and Nelson, W.J. (1994) *J. Cell Biol.* 125, 1327–1340.
- [19] Weiss, E.E., Kroemker, M., Rüdiger, A.H., Jockusch, B.M. and Rüdiger, M. (1998) *J. Cell Biol.* 141, 755–764.
- [20] Hüttelmaier, S., Bubeck, P., Rüdiger, M. and Jockusch, B.M. (1997) *Eur. J. Biochem.* 247, 1136–1142.
- [21] Stafford, W.F.I., Mabuchi, K., Takahashi, K. and Tao, T. (1995) *J. Biol. Chem.* 270, 10576–10579.
- [22] Haffner, C., Jarchau, T., Reinhard, M., Hoppe, J., Lohmann, S.M. and Walter, U. (1995) *EMBO J.* 14, 19–27.
- [23] Takeuchi, K., Takahashi, K., Abe, M., Nishida, W., Hiwada, K., Nabeya, T. and Maruyama, K. (1991) *J. Biochem.* 109, 311–316.
- [24] North, A.J., Gimona, M., Cross, R.A. and Small, J.V. (1994) *J. Cell Sci.* 107, 445–455.